Parameter-Varying Hydrodynamic Model of a Single Vane in a Variable-Geometry Oscillating Surge Wave Energy Converter

Preprint

Tania Demonte Gonzalez,[1] Nathan Tom,[2] and Gordon G. Parker[1]

1 Michigan Technological University
2 National Renewable Energy Laboratory

Presented at 2024 American Control Conference
Toronto, Canada
July 10–12, 2024

NREL is a national laboratory of the U.S. Department of Energy
Office of Energy Efficiency & Renewable Energy
Operated by the Alliance for Sustainable Energy, LLC

This report is available at no cost from the National Renewable Energy Laboratory (NREL) at www.nrel.gov/publications.

Contract No. DE-AC36-08GO28308

Conference Paper
NREL/CP-5700-87548
July 2024

Parameter-Varying Hydrodynamic Model of a Single Vane in a Variable-Geometry Oscillating Surge Wave Energy Converter

Preprint

Tania Demonte Gonzalez,[1] Nathan Tom,[2] and Gordon G. Parker[1]

1 Michigan Technological University
2 National Renewable Energy Laboratory

Suggested Citation
Demonte Gonzalez, Tania, Nathan Tom, and Gordon G. Parker. 2024. *Parameter-Varying Hydrodynamic Model of a Single Vane in a Variable-Geometry Oscillating Surge Wave Energy Converter: Preprint*. Golden, CO: National Renewable Energy Laboratory. NREL/CP-5700-87548. https://www.nrel.gov/docs/fy24osti/87548.pdf.

NREL is a national laboratory of the U.S. Department of Energy
Office of Energy Efficiency & Renewable Energy
Operated by the Alliance for Sustainable Energy, LLC

This report is available at no cost from the National Renewable Energy Laboratory (NREL) at www.nrel.gov/publications.

Contract No. DE-AC36-08GO28308

Conference Paper
NREL/CP-5700-87548
July 2024

National Renewable Energy Laboratory
15013 Denver West Parkway
Golden, CO 80401
303-275-3000 • www.nrel.gov

NOTICE

This work was authored in part by the National Renewable Energy Laboratory, operated by Alliance for Sustainable Energy, LLC, for the U.S. Department of Energy (DOE) under Contract No. DE-AC36-08GO28308. Funding provided by U.S. Department of Energy Office of Energy Efficiency and Renewable Energy Water Power Technologies Office. The views expressed herein do not necessarily represent the views of the DOE or the U.S. Government. The U.S. Government retains and the publisher, by accepting the article for publication, acknowledges that the U.S. Government retains a nonexclusive, paid-up, irrevocable, worldwide license to publish or reproduce the published form of this work, or allow others to do so, for U.S. Government purposes.

This report is available at no cost from the National Renewable Energy Laboratory (NREL) at www.nrel.gov/publications.

U.S. Department of Energy (DOE) reports produced after 1991 and a growing number of pre-1991 documents are available free via www.OSTI.gov.

Cover Photos by Dennis Schroeder: (clockwise, left to right) NREL 51934, NREL 45897, NREL 42160, NREL 45891, NREL 48097, NREL 46526.

NREL prints on paper that contains recycled content.

Parameter-Varying Hydrodynamic Model of a Single Vane in a Variable-Geometry Oscillating Surge Wave Energy Converter

Tania Demonte Gonzalez[1], Nathan Tom[2] and Gordon G. Parker[1]

***Abstract*— This paper presents a preliminary study on the parameter-varying hydrodynamic modeling of an individual vane of a variable-geometry oscillating surge wave energy converter (VGOSWEC). The WEC design incorporates controlled surfaces that can modify their orientation relative to the wave motion, reducing hydrodynamic pressure and related loads. This research focuses on characterizing the behavior of the oscillating WEC using a simplified model and three methods for achieving a continuous parameter-varying model: coarse hydrodynamic parameters, interpolation of hydrodynamic parameters, and a fitting function. The results of this study contribute to the understanding of parameter-varying hydrodynamic effects in variable geometry oscillating WECs. The findings provide insights into the potential for reducing structural loads and improving the overall performance of such devices. Further research and development in this area could lead to advancements in WEC technologies, enabling their integration into the competitive energy market.**

I. Introduction

Wave Energy Converters (WECs) are devices designed to harness the kinetic energy of ocean waves and convert it into useful forms of energy, such as electricity. There are various types of WECs, but they all share a fundamental working principle: the utilization of a mechanical system known as the Power Take-Off (PTO) system to transform wave energy into useful power.

During the past decades, researchers have been focusing on reducing the levelized cost of energy (LCOE) to advance WEC technologies from government-funded research to the competitive energy market. Much effort has been put into optimizing PTO designs and control strategies to minimize LCOE. However, one of the major cost drivers in WECs is the structural components [1], which account for approximately 37-52% of the LCOE, while the PTO is estimated to contribute around 8% [2]. Hence, in order to achieve a significant reduction in LCOE, it is essential to optimize the structural design. Oscillating surge WEC (OSWEC) devices are designed to be deployed near shore, where they must withstand extreme sea conditions that result in increases in structural loads. Therefore, the potential reductions in LCOE might only be accomplished once the WEC structure incorporates an enhanced load-shedding capability.

*This work was supported by the U.S. Department of Energy under Contract No. DE-AC36-08GO28308 with the National Renewable Energy Laboratory. Funding for the work was provided by the DOE Office of Energy Efficiency and Renewable Energy, Wind and Water Power Technologies Office

[1]Mechanical Engineering-Engineering Mechanics, Michigan Technological University, Houghton, MI 49931, USA tsdemont@mtu.edu, ggparker@mtu.edu

[2]National Renewable Energy Laboratory, Golden, CO 80401, USA nathan.tom@nrel.gov

In recent studies, researchers at the National Renewable Energy Laboratory (NREL) have developed a novel WEC that combines a surge wave energy converter with controlled surfaces [3], [4]. The proposed design incorporates identical actuated vanes to the general shape of a traditional OSWEC. The main flap is hinged at the bottom and holds four ellipsoid vanes that can rotate as shown in Fig. 1, resulting in a variable-geometry oscillating surge wave energy converter (VGOSWEC). The device has the capability to modify the surfaces perpendicular to the motion of the waves, resulting in a decrease in hydrodynamic pressure and related loads.

Several authors have explored various aspects of this novel VGOSWEC. For instance, Tom et al. [5] developed a pseudo-spectral control algorithm to maximize energy and reduce loads of a VGOSWEC, Huseain et al. [6] investigated the impact on the performance by elevating the VGOSWEC structure, and Choiniere et al. [7] conducted experimental testing on the VGOSWEC to analyze the difference in hydrodynamics when compared to a traditional OSWEC. These studies have demonstrated the potential of VGOSWEC to reduce loads when the device transitions from power production mode to survival mode. Here, survival mode refers to the operational state when the OSWEC shelters itself to prevent damage or failure rather than generating power.

In the papers aforementioned, the authors have primarily modeled the VGOSWEC using linear hydrodynamic models with a static configuration of the vanes. This research presents a preliminary investigation focused on characterizing the behavior of the VGOSWEC using continuous parameter-varying models, where the hydrodynamic parameters vary dynamically with the vane position.

Considering the investigative scope of this study, a simplified model focusing on a singular vane of the VGOSWEC is adopted. Previous research has developed configuration-dependent models like in [8], [9], and [10]. Similar methods are employed in this work to develop parameter-varying models based on multiple linear time-invariant (LTI) models obtained for various vane positions [11]. Three distinct methods are used to create continuous parameter-varying models. The first method involves switching between the coarse hydrodynamic parameters obtained from the boundary element method (BEM) solver WAMIT [12] based on the vane rotation. The second method interpolates the hydrodynamic parameters across the rotation of the vane at a finer angle increment. Finally, the third method uses a function for the hydrodynamic coefficients using a least-squares fit. All methods are analyzed and compared to a traditional LTI

This report is available at no cost from the National Renewable Energy Laboratory at www.nrel.gov/publications.

model with a static vane for different regular waves.

The paper is organized as follows. Section II describes the derivation of the hydrodynamic models, Section III shows the results of the simulation, and finally, Section IV presents the conclusion and future work.

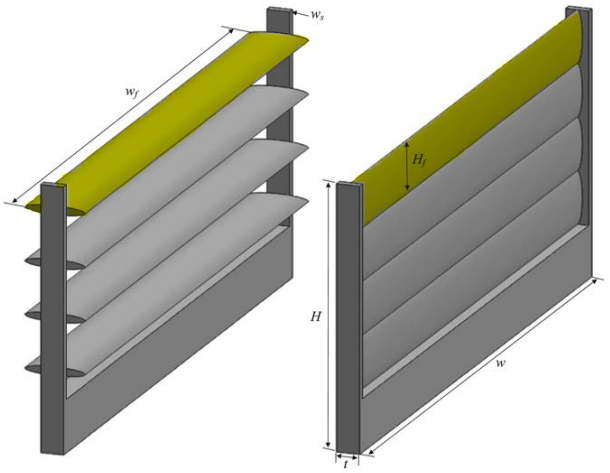

Fig. 1. Oscillating wave energy converter with controllable surfaces with individual vane modeled highlighted. [3]

II. Hydrodynamic Modeling

The rotating vane is a one-degree-of-freedom system that can be modeled as an oscillating surge WEC; however, instead of being hinged at the bottom like traditional OSWECs, the vane is hinged in the center of the geometry and can therefore complete full rotations. The general equation of motion in the time domain can be described using Newton's second law:

$$I\ddot{\zeta} = \tau_e + \tau_r + \tau_h + \tau_m \tag{1}$$

where I is the vane's constant mass moment of inertia about its rotation axis whose geometric parameters are given in Table I. The vane angular acceleration is denoted $\ddot{\zeta}$, τ_e is the excitation torque caused by the incident waves, τ_r is the wave radiation torque due to pitch motion, τ_h is the hydrostatic restoring torque, and τ_m is the applied mechanical torque.

For small rotations from a linearized orientation, the hydrostatic restoring torque can be described as:

$$\tau_h = -C(\zeta)\,\zeta \tag{2}$$

where C is the hydrostatic restoring coefficient, which is obtained using WAMIT [12] for vane angles ranging from 0° to 90°.

The Cummins equation [13] is used to represent the linear hydrodynamic wave radiation torque in the time domain, and it can be expressed as:

$$\tau_r = -\mu_\infty(\zeta)\ddot{\zeta} - \int_0^t K_r(\zeta, t-\tau)\dot{\zeta}(\tau)d\tau \tag{3}$$

where $\mu_\infty(\zeta)$ is the pitch added mass moment of inertia at infinite frequency, and $K_r(\zeta)$ is the pitch radiation impulse response function (IRF). Like C, they were both computed for a range of vane angles.

The excitation torque is

$$\tau_e = \int_{-\infty}^{\infty} K_e(\zeta, t-\tau)\,\eta(\tau)\,d\tau \tag{4}$$

where η is the wave elevation and $K_e(\zeta)$ is the excitation torque IRF that was also computed for a range of ζ values. A torsional spring was implemented at each vane given by Equation 5.

$$\tau_m = -k_m\,\zeta \tag{5}$$

where k_m is the spring stiffness coefficient. Combining Equations (1)–(5), the resulting one-degree-of-freedom pitch equation of motion is:

$$\begin{aligned}[I + \mu_\infty(\zeta)]\,\ddot{\zeta} = -C(\zeta)\zeta - \int_0^t K_r(\zeta, t-\tau)\dot{\zeta}(\tau)d\tau \\ + \int_{-\infty}^{\infty} K_e(\zeta, t-\tau)\eta(\tau)d\tau - k_m\,\zeta\end{aligned} \tag{6}$$

TABLE I
Geometric parameters of a single controllable surface.

Water Depth	10.00 m
Vane Minor Axis	0.33 m
Vane Major Axis	2.00 m
Vane Width	4.50 m
Moment of Inertia, I	672.7 kg

In summary, the configuration-dependent hydrodynamic parameters $\mu_\infty(\zeta)$, $C(\zeta)$, $K_r(\zeta)$, and $K_e(\zeta)$ vary due to changes in vane angle ζ. They were obtained for 18 vane angles from 0° to 90° and interpolated during simulation at intermediate points. This modeling approach assumes certain flow conditions that deviate from traditional BEM solvers like WAMIT. However, the primary objective of this study is to assess the potential consequences that may arise when combining LTI models using interpolation and curve fitting. Previous studies have shown that there is a noticeable reduction in these hydrodynamic coefficients when comparing the 0° configurations with all other configurations [6], [7]. This has been attributed to the decrease in pressure exerted on the vane as it opens and allows more flow.

The change in τ_r and τ_e is most significant between 0° and 20°, which is illustrated in Fig. 3 , via the radiation damping coefficient $b(\zeta, \omega)$ associated with $K_r(\zeta)$ through Equation (7) [14]. Therefore, $K_r(\zeta)$ and $K_e(\zeta)$ were obtained from 0° to 20° every 2°, and from 20° to 90° every 10°. The fine angles vane rotations in the $\pm 20^\circ$ range are represented by dash-dot lines while the coarse range of angles every 10° is represented with a solid line. This figure shows the decrease in amplitude of the radiation coefficient as the vane transitions from a fully closed ($\zeta = 0^\circ$) to a fully open configuration ($\zeta = 90^\circ$). Moreover, within the $\pm 20^\circ$ range, there is a distinct, rapid variation in the radiation coefficient.

This report is available at no cost from the National Renewable Energy Laboratory at www.nrel.gov/publications.

$$b(\zeta,\omega) = \int_0^\infty K_r(\zeta, t-\tau)\cos\omega d\tau \tag{7}$$

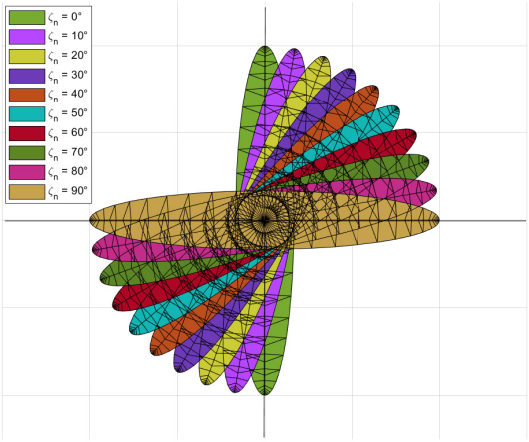

Fig. 2. Mesh of the modeled vane at discrete angles ζ every $10°$.

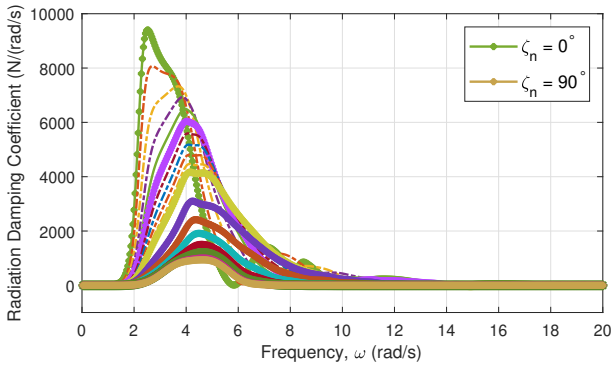

Fig. 3. Radiation Damping Coefficient $b(\zeta,\omega)$ at different vane angles. The coefficients of ζ every $10°$ is represented with a solid and marker line and the coefficients for ζ every $2°$ in the $\pm 20°$ range are represented with a dash-dot line.

A. Parameter Interpolation

Under regular waves, all of the hydrodynamic parameters that depend on ζ can be linearly interpolated between grid points. The variation of $\mu_\infty(\zeta)$ and $C(\zeta)$ are symmetric about $\zeta = 0°$ as the vane pitch angle changes. Interpolation was done in MATLAB using *interp1* for a fine range of ζ from $0°$ to $90°$ with an increment of $0.5°$ forming a one-dimensional table lookup.

The radiation torque can be approximated using a state-space model to include the transient dynamics [15]. The Fourier transform of the wave radiation IRF τ_r at each pitch angle can be represented as

$$\begin{aligned} K_{R,n}(i\omega) &= \frac{B_{R,n}(i\omega)}{A_{R,n}(i\omega)} \\ &= \frac{\sum_{k=1}^{q_R(n)} b_{R,n,k}(i\omega)^{q_R(n)-k}}{(i\omega)^{q_R(n)} + \sum_{k=1}^{q_R(n)} a_{R,n,k}(i\omega)^{q_R(n)-k}} \\ where \quad n &= 1, 2, ...N \end{aligned} \tag{8}$$

where $A_{R,n}(i\omega)$ and $B_{R,n}(i\omega)$ are the denominator and numerator polynomials, respectively, of the wave radiation kernel of which $a_{R,n,k}(i\omega)$ and $b_{R,n,k}(i\omega)$ are the respective coefficients, and $q_R(n)$ is the order of the wave radiation IRF Fourier transfer function at pitch angle ζ_n.

Similarly, the wave exciting torquecan be represented as the set of the Fourier transforms functions $K_{E,n}(i\omega)$ of the wave-excitation moment IRF τ_e .

The coefficients of $K_{R,n}(i\omega)$ and $K_{E,n}(i\omega)$ are derived using the identification scheme based on Hankel singular value decomposition (SVD) [16], which is available in the MATLAB function *imp2ss*. This function has a limitation regarding the ability to select the state-space order manually. Therefore, a model reduction technique was employed using the MATLAB function *balred*.

The configuration-dependent coefficients of the wave-excitation and wave-radiation IRFs were obtained by interpolating the coefficients of the corresponding sets of Fourier transforms, $K_{E,n}(i\omega)$ and $K_{R,n}(i\omega)$, respectively. In the case of the wave-radiation IRF, the orders of the transfer function numerator and denominator remain constant for all pitch angles ζ, denoted as $q_R(n) = 6$.

The excitation torque τ_e is not symmetric about $\zeta = 0°$ since there is a change in the phase of the excitation moment depending on the vane position. In addition, the wave-exciting torque IRF K_e in Equation (4) is non-causal, requiring the computation of this term to be done separately from the rest of the simulation. Therefore, the excitation torque was evaluated at each ζ for different wave elevations, which were then interpolated across the different pitch angles ζ and time t, forming a 2D lookup table. The range of ζ was considered from $-90°$ to $90°$, and the interpolation was done every $0.5°$. The excitation moment surface for a regular wave of amplitude 1.5 m and frequency of 1 rad/s is shown in Fig. 4. In this figure, it can be observed from (a) that the greatest change in amplitude of τ_e occurs between $\pm 20°$, and from (b) the change in the phase of the excitation moment. Note that to avoid large transient responses on the excitation moment, the simulation included a ramp of 25 seconds on the input wave elevation. The interpolated excitation moment is used for both the interpolated and the curve fit method.

B. Least-squares fitting functions

The interpolated parameter-varying model developed has the advantage of being more accurate when compared to the coarse parameter-varying model; however, due to the large size of table look-ups for each hydrodynamic parameter, it results in a more computationally expensive model. Therefore,

This report is available at no cost from the National Renewable Energy Laboratory at www.nrel.gov/publications.

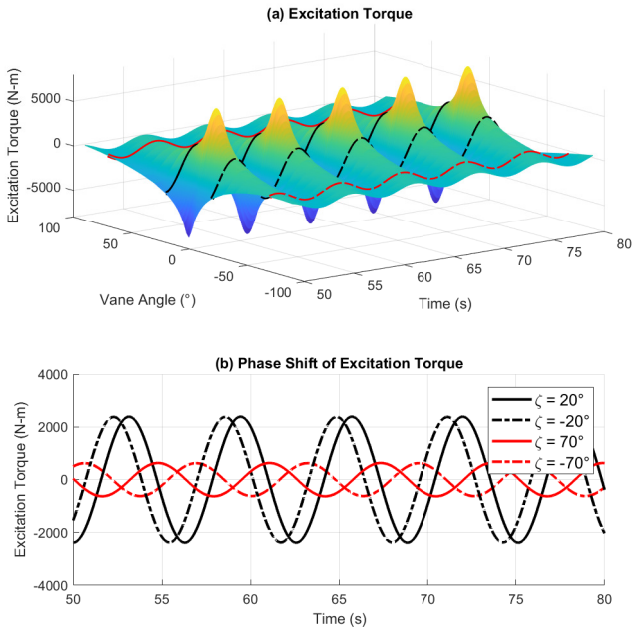

Fig. 4. Excitation torque for a wave $\eta(t) = 1.5sin(t)$.

a third model was developed where the PV hydrodynamic parameters are functions of the pitch angle ζ.

The curve fitting was done using *polyfit* in MATLAB. This function uses the least-squares method to fit a polynomial curve to data points. It calculates the Vandermonde matrix, solves a linear system of equations, and finds the polynomial coefficients that minimize the sum of squared residuals resulting in the least-squares best curve fit.

The changes in $\mu_\infty(\zeta)$ and $C(\zeta)$ with respect to the pitch angle are symmetric around $\zeta = 0°$ [9]; hence, the fitting function can be expressed using the absolute value of ζ. The polynomial order is 6 for both $\mu_\infty(t)$ and $C(t)$.

Similarly, a fixed-order fit was used for each of the coefficients of the numerator B_R and denominator A_R in Equation (8) across all ζ. The polynomials are expressed as:

$$a_{R,r}(t) = \sum_{k=0}^{N(Ar)} p_{Ar,k}|\zeta(t)|^{N(Ar)-k} \tag{9}$$

and

$$b_{R,r}(t) = \sum_{k=0}^{N(Br)} p_{Br,k}|\zeta(t)|^{N(Br)-k} \tag{10}$$

where N_{Ar} and N_{Br} are the order of each polynomial, and p_{Ar} and p_{Br} are the respective polynomial coefficients. Fig. 5 shows the interpolation and curve-fitted function of the 7th coefficient of Equations (9) and (10). It is easy to observe from this figure the significant change of the coefficients between the region of $\pm 20°$. This trend is also observed in the rest of the coefficients.

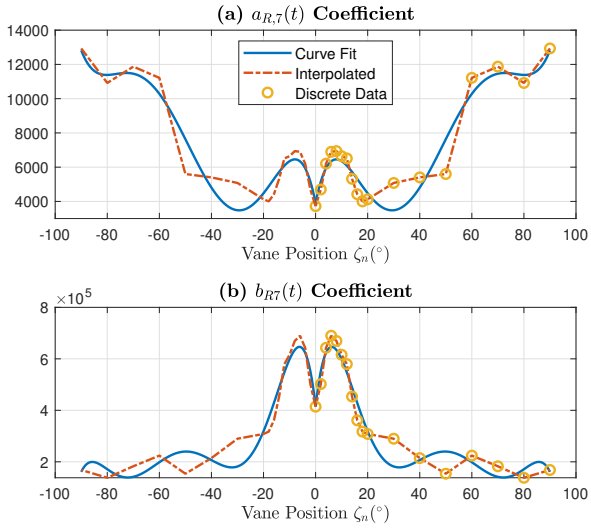

Fig. 5. 7th coefficient of the radiation transfer function for each ζ and their interpolation and curve-fitted function.

III. Results

The simulation was run for different regular wave profiles comparing differences between the LTI and the three parameter-varying models: coarse, interpolation, and curve fit. The hydrodynamic parameters used for the LTI model were those corresponding to a fully closed vane configuration at $\zeta = 0°$.

To characterize the effect of the incident wave amplitude and frequency on the total hydrodynamics and the response of the oscillating vane, three results are shown. The first two cases have the same wave frequency, but the amplitude is 0.5 m for the first case, and 4 m for the second case. These results are plotted in Fig. 6 and Fig. 7 respectively, and they depict the effect of increasing the wave amplitude at a low wave frequency of 0.5 rad/s. The third case, shown in Fig. 8, is the response of the vane to a higher frequency wave at 1.5 rad/s for the same wave amplitude as the first case of 0.5 m.

The total hydrodynamic torque τ_T is the sum of all the terms on the right-hand side of Equation (6) besides the mechanical torque τ_m:

$$(I + \mu_\infty(\zeta))\ddot{\zeta} = \tau_T - k_m\zeta \tag{11}$$

The mechanical spring coefficient k_m was adjusted accordingly to each wave elevation to prevent vane rotations outside the $\pm 90°$ range. For the first case $k_m = 5$ kNm/rad, for the second case $k_m = 10$ kNm/rad, and for the third case $k_m = 15$ kNm/rad.

The results in Fig. 6 show the difference in the vane rotation, total hydrodynamic torque, and mechanical torque when comparing the LTI model with PV models. In scenarios with minimal wave elevation, the difference in the amplitude of the rotation of the vane is not very significant. When comparing the PV models, the interpolated and curve fit results are near-identical, whereas a noticeable contrast is seen with the coarse PV model.

This report is available at no cost from the National Renewable Energy Laboratory at www.nrel.gov/publications.

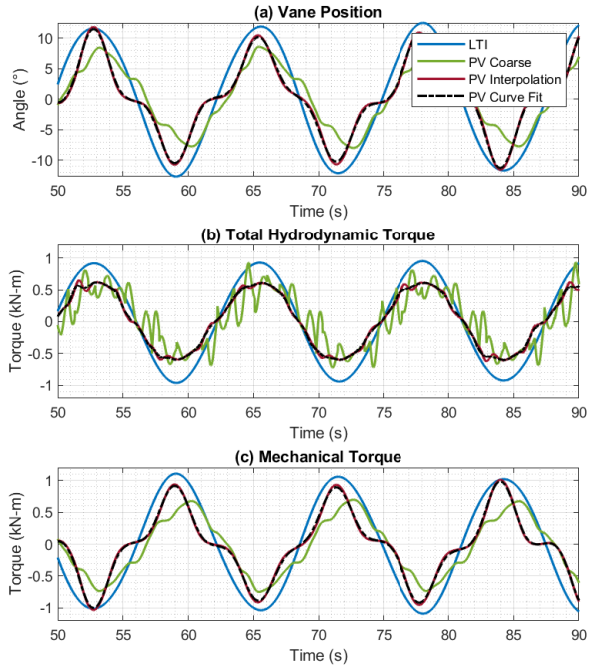

Fig. 6. Simulation results for a low frequency $\omega = 0.5$ rad/s and low amplitude $\alpha = 0.5$ m wave elevation with $k_m = 5$ kN m/rad.

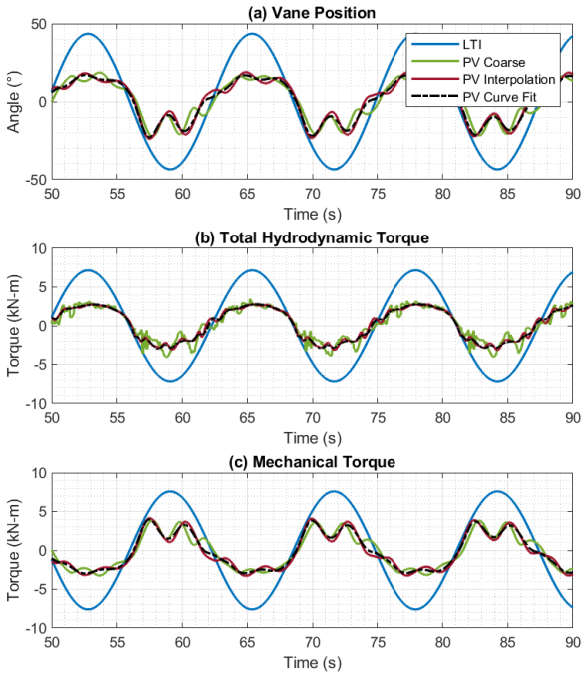

Fig. 7. Simulation results for a low frequency $\omega = 0.5$ rad/s and high amplitude $\alpha = 4$ m wave elevation with $k_m = 10$ kN m/rad

The interpolated and curve fit models are similar because they both implement the same interpolated excitation moment, which represents the primary contributor to the total hydrodynamic torque. The PV coarse model results, on the other hand, present higher frequency content on the total hydrodynamic torque compared to the other models. This is attributed to the substantial shift in hydrodynamic parameters within the $\pm 20^\circ$ range, leading to more pronounced transients in the radiation term and larger peaks on the excitation moment.

The second case examines how the vane responds and how the hydrodynamic torque changes to a high-amplitude wave. As illustrated in Fig. 7, a significant difference becomes evident between the LTI model and the PV models. This suggests that employing the LTI model for significant wave conditions would lead to substantial inaccuracies in the dynamic model. The non-sinusoidal response of the vane of the PV models is mainly due to the shift in phase of the wave excitation torque. Additionally, Fig. 7 demonstrates that the total hydrodynamic torque experienced by the rotating vane is potentially much lower than that experienced by a fully closed vane, resulting in the desired load-shedding behavior for high-amplitude waves.

Both the interpolated and curve fit models yield remarkably similar results, with the primary distinction being in computational demands. The interpolated model uses extensive and computationally expensive lookup tables for all parameter-varying parameters, whereas the curve-fitting model relies on functions to estimate these parameters.

The final case, depicted in Fig. 8, explores the system's response to low-amplitude, high-frequency waves. Similar to the previous case, there is a notable disparity between the LTI model and the PV models. The total torque of the coarse model exhibits a significant amount of high-frequency content attributed to the radiation force. It is important to note that the coarse model's similarity to the interpolated and curve fit methods is attributed to the use of finer discretization angles in the high-transition region of hydrodynamic parameters. Otherwise, this model's performance would not be as favorable.

IV. Conclusion

This study provides valuable insights into the dynamics of the VGOSWEC through the application of continuous parameter-varying hydrodynamic models. VGOSWECs hold significant promise in advancing wave energy conversion technology, particularly in the quest to reduce the LCOE [4].

The research shows that the traditional LTI model, while suitable for some scenarios, tends to exhibit inaccuracies, particularly when confronted with significant wave conditions. This highlights the critical importance of employing parameter-varying models in capturing the behavior of VGOSWECs under varying wave amplitudes and frequencies when evaluating the trade-offs of pursuing real-time control of variable geometry modules.

Three parameter-varying models were analyzed: a coarse model, an interpolated model, and a curve fit model. The

This report is available at no cost from the National Renewable Energy Laboratory at www.nrel.gov/publications.

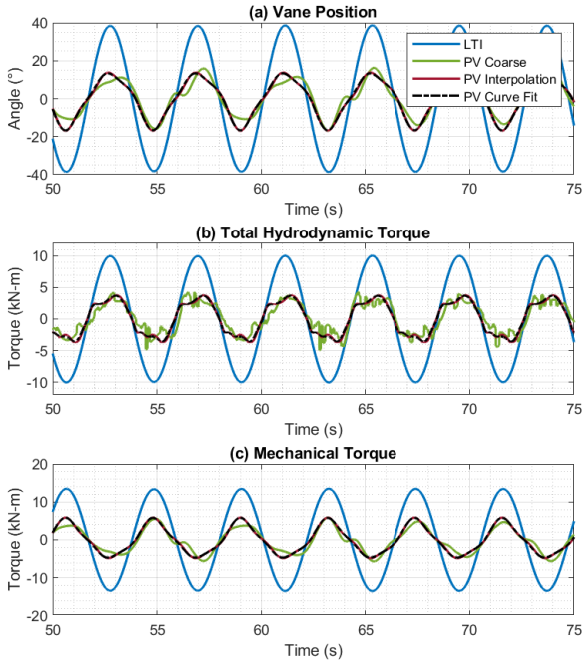

Fig. 8. Simulation results for a high frequency $\omega = 1.5(rad/s)$ and low amplitude $\alpha = 0.5m$ wave elevation with $k_m = 15(kNm/rad)$

interpolated and curve fit models demonstrated remarkable similarity, primarily attributed to the use of the same interpolated excitation moment, a significant contributor to the total hydrodynamic torque. Meanwhile, the coarse model exhibited a higher frequency content, due to the abrupt change in the values of the hydrodynamic parameters within a specific vane angle range. The results of this study highlight the potential benefits of VGOSWEC technology, particularly in load-shedding behavior under high-amplitude and high-frequency waves. This behavior, observed as a substantial reduction in the total hydrodynamic torque, has the capacity to significantly reduce the costs associated with oscillating surge converters. While the study employed a simplified model, it paves the way for more sophisticated modeling approaches where all of the vanes of the VGOSWEC are included.

Future research on this topic should focus on refining these models, verification of the models against a high-fidelity model, and finally, validation of the models through practical implementation to accelerate the development of VGOSWEC technology in real-world marine environments. Additional control strategies on the mechanical torque could be further explored to create combinations of vane rotations that yield the most load-shedding behavior in survival mode and the most power extraction in power production mode. The control strategies that could be implemented would be similar to those applied in OSWECs for power production [17].

ACKNOWLEDGMENT

This work was authored in part by the National Renewable Energy Laboratory, operated by Alliance for Sustainable Energy, LLC, for the U.S. Department of Energy (DOE) under Contract No. DE-AC36-08GO28308. Funding provided by the U.S. Department of Energy Office of Energy Efficiency and Renewable Energy Water Power Technologies Office. The views expressed in the article do not necessarily represent the views of the DOE or the U.S. Government. The U.S. Government retains and the publisher, by accepting the article for publication, acknowledges that the U.S. Government retains a nonexclusive, paid-up, irrevocable, worldwide license to publish or reproduce the published form of this work, or allow others to do so, for U.S. Government purposes.

REFERENCES

[1] Y. H. Yu, D. S. Jenne, R. Thresher, A. Copping, S. Geerlofs, and L. A. Hanna, "Reference Model 5 (RM5): Oscillating Surge Wave Energy Converter," Tech. Rep. NREL/TP–5000-62861, 1169778, Jan. 2015.

[2] D. S. Jenne, Y. H. Yu, and V. Neary, "Levelized Cost of Energy Analysis of Marine and Hydrokinetic Reference Models: Preprint," Tech. Rep. NREL/CP-5000-64013, National Renewable Energy Lab. (NREL), Golden, CO (United States), Apr. 2015.

[3] N. Tom, M. Lawson, Y.-H. Yu, and A. Wright, "Spectral modeling of an oscillating surge wave energy converter with control surfaces," *Applied Ocean Research*, vol. 56, pp. 143–156, Mar. 2016.

[4] N. M. Tom, M. J. Lawson, Y. H. Yu, and A. D. Wright, "Development of a nearshore oscillating surge wave energy converter with variable geometry," *Renewable Energy*, vol. 96, pp. 410–424, Oct. 2016.

[5] N. M. Tom, Y. H. Yu, A. D. Wright, and M. J. Lawson, "Pseudo-spectral control of a novel oscillating surge wave energy converter in regular waves for power optimization including load reduction," *Ocean Engineering*, vol. 137, pp. 352–366, June 2017.

[6] S. Husain, J. Davis, N. Tom, K. Thiagarajan, C. Burge, and N. Nguyen, "Influence on Structural Loading of a Wave Energy Converter by Controlling Variable-Geometry Components and the Power Take-Off: Preprint," *Renewable Energy*, 2022.

[7] M. Choiniere, J. Davis, N. Nguyen, N. Tom, M. Fowler, and K. Thiagarajan, "Hydrodynamics and load shedding behavior of a variable-geometry oscillating surge wave energy converter (OSWEC)," *Renewable Energy*, vol. 194, pp. 875–884, July 2022.

[8] L. Papillon, L. Wang, N. Tom, J. Weber, and J. Ringwood, "Parametric modelling of a reconfigurable wave energy device," *Ocean Engineering*, vol. 186, p. 106105, Aug. 2019.

[9] A. P. McCabe, G. A. Aggidis, and T. J. Stallard, "A time-varying parameter model of a body oscillating in pitch," *Applied Ocean Research*, vol. 28, pp. 359–370, Dec. 2006.

[10] D. Crooks, *Nonlinear hydrodynamic modelling of an oscillating wave surge converter*. PhD thesis, July 2017.

[11] R. Murray-Smith and T. Johansen, *Multiple Model Approaches To Nonlinear Modelling And Control*. CRC Press, 1997. Google-Books-ID: XgoHEAAAQBAJ.

[12] "Wamit, Inc. - The State of the Art in Wave Interaction Analysis."

[13] W. Cummins and U. S. Navy, *The Impulse Response Functions and Ship Motions*. David Taylor Model Basin, United States Department of the Navy, David Taylor Model Basin, 1962.

[14] T. F. Ogilvie, "Recent progress toward the understanding and prediction of ship motions," *David W. Taylor Model Basin, Washington D.C., USA, Presented at: Proceedings of the 5th Symposium on Naval Hydrodynamics, Bergen, Norway, pp. 3-80*, 1964.

[15] E. Kristiansen and O. Egeland, "Frequency-Dependent Added Mass in Models for Controller Design for Wave Motion Damping," *IFAC Proceedings Volumes*, vol. 36, pp. 67–72, Sept. 2003.

[16] S. Kung, "A new identification and model reduction algorithm via singular value decomposition," 1978.

[17] A. Maria-Arenas, A. J. Garrido, E. Rusu, and I. Garrido, "Control Strategies Applied to Wave Energy Converters: State of the Art," *Energies*, vol. 12, p. 3115, Jan. 2019. Number: 16 Publisher: Multidisciplinary Digital Publishing Institute.

This report is available at no cost from the National Renewable Energy Laboratory at www.nrel.gov/publications.